

K. Schmid, K. Krieger, S. W. Lisgo, S. Brezinsek
and JET EFDA contributors

WALLDYN Simulations of Global Impurity Migration and Fuel Retention in JET and Extrapolations to ITER

“This document is intended for publication in the open literature. It is made available on the understanding that it may not be further circulated and extracts or references may not be published prior to publication of the original when applicable, or without the consent of the Publications Officer, EFDA, Culham Science Centre, Abingdon, Oxon, OX14 3DB, UK.”

“Enquiries about Copyright and reproduction should be addressed to the Publications Officer, EFDA, Culham Science Centre, Abingdon, Oxon, OX14 3DB, UK.”

The contents of this preprint and all other JET EFDA Preprints and Conference Papers are available to view online free at www.iop.org/Jet. This site has full search facilities and e-mail alert options. The diagrams contained within the PDFs on this site are hyperlinked from the year 1996 onwards.

WALLDYN Simulations of Global Impurity Migration and Fuel Retention in JET and Extrapolations to ITER

K. Schmid¹, K. Krieger¹, S. W. Lisgo², S. Brezinsek^{3,4}
and JET EFDA contributors*

JET-EFDA, Culham Science Centre, OX14 3DB, Abingdon, UK

¹*Max-Planck-Institut für Plasmaphysik, Boltzmannstraße 2, D-85748 Garching, Germany*

²*ITER Organization, Route de Vinon sur Verdon, 13115 Saint Paul-lez-Durance, France*

³*Institute of Energy and Climate Research – Plasma Physics, Forschungszentrum Jülich,
52425 Jülich, Germany*

⁴*JET-EFDA, Culham Science Centre, Abingdon, OX14 3DB, UK*

** See annex of F. Romanelli et al, “Overview of JET Results”,
(25th IAEA Fusion Energy Conference, St Petersburg, Russia (2014)).*

ABSTRACT:

The migration of first wall material due to erosion, plasma transport and re-deposition is one of the key challenges in current and future fusion devices. To predict erosion/re-deposition patterns and to understand the underlying principal processes, the global simulation code WallDYN was developed. It couples the evolution of the first wall surface composition to plasma impurity transport. To benchmark the WallDYN model, it was applied to the JET ITER-Like Wall experiment (JET-ILW), which mimics the ITER first wall material configuration and is thus an ideal environment to validate the predictive significance of WallDYN calculations for ITER application. The WallDYN calculations show good qualitative agreement with the Be deposition patterns determined from JET-ILW post-campaign wall tile analysis. A comparison of the calculated retention results for C and Be first wall configurations with the experimental results even shows a quantitative agreement when long term outgassing is taken into account. Applying the same model and process physics as for the JET calculations, the impurity migration and resulting fuel species co-deposition in ITER for different wall configurations and background plasmas was calculated. The simulations show that C containing wall configurations lead to unacceptable T retention whereas for the current ITER material choice (Be wall & W divertor) co-deposition will not limit the ITER operation.

1. INTRODUCTION

The migration of first wall material due to erosion, plasma transport and deposition is one of the key challenges in current and future fusion devices. It affects the lifetime of wall components in net erosion regions and can lead to formation of mixed material layers and strong fuel retention via co-deposition in net deposition regions of the first wall. To predict erosion/(re-)deposition patterns and to understand the underlying principal processes, a global simulation code is required that couples the evolution of the first wall surface composition to plasma impurity transport. To that end, the WallDYN [1] code was developed. It maintains a strict global material balance of all eroded and (re-)deposited material and allows the tracking of the chain of subsequent erosion/(re-)deposition/re-erosion steps that define where material is finally net-deposited or net-eroded. WallDYN couples state of the art models for the surface processes (e.g. erosion, reflection, implantation, sublimation) with material redistribution data from trace impurity plasma transport models in a fully self-consistent simulation. For each plasma exposed location on the discretized first wall contour it calculates the time evolution of both the composition of elements in the surface and in the incident particle flux. The fuel retention rate via co-deposition can be derived from the calculated layer growth rate by multiplying with the hydrogen concentration in the layer, which can be taken from scaling laws fitted to lab experiments [3].

To benchmark the WallDYN model, it was applied to the JET ITER-Like Wall experiment (JET-ILW), which mimics the ITER first wall material configuration and is thus an ideal environment to validate the predictive significance of the WallDYN deposition/retention calculations for

ITER application. To calculate Be deposition patterns that can be compared with the measured distribution of deposited Be in [4, 5], WallDYN simulations were performed for L-mode and H-mode plasma scenarios used in global retention studies both during the JET-ILW campaigns and previous JET-Carbon (JET-C) campaigns. This allowed quantitative validation of the code predictions against the strong difference in deposition patterns & global fuel retention between the C- and Be-dominated JET configurations.

Applying the same model and process physics as for the JET calculations, the Be deposition patterns and resulting fuel species co-deposition in ITER for different wall configurations and background plasmas was calculated. The background plasmas used in DIVIMP to calculate the redistribution information span a large range of plasma parameters at the wall.

In addition to (co-)deposition WallDYN also calculates the erosion rate for all wall elements. For ITER the erosion of W is a key parameter since excessive W sputtering could severely limit the operational space due to the tendency of W to accumulate and radiate in the plasma core. The paper will first present some of the JET-ILW WallDYN benchmarking calculations, showing that WallDYN achieves a reasonable match of current available experimental data on Be deposition and fuel retention by co-deposition. Then the predictions for ITER w.r.t Be deposition and fuel retention by co-deposition will be discussed. Finally some results on the erosion of W by self-sputtering will be presented.

2. MODEL DESCRIPTION

The WallDYN model is described in detail in [1, 2] therefore only a short summary of the main concepts is given here.

WallDYN discretizes the wall into N-wall elements and calculates the time evolution of the surface composition and the incident particle spectrum on each wall element due erosion, deposition and global particle transport.

The surface composition is described by the areal densities $\delta_{ei,wk} (m^{-2})$ of the species ei in on each wall element wk . The surface composition evolution is determined from a differential equation describing the flux balance of material loss (erosion & sublimation $\Gamma_{ei,wk}^{ERO}$) and gain (deposition $\Gamma_{ei,wk}^{DEP}$) due to the local incident particle spectrum. The rate determining parameters (erosion & reflection yield, sublimation rate) for the surface composition evolution are calculated from scaling laws. These scaling laws are determined from fits to experimental data and output from state of the art models (e.g. SDTRIM.SP [10, 11]).

The incident particle spectrum is given the flux $\Gamma_{ej,wl}$ of element ej on wall element wl ($m^{-2}s^{-1}$). The incident flux evolution is calculated from the fluxes from each wall element into the plasma due to reflection & erosion multiplied by the material re-distribution matrix. This redistribution matrix is a parametrization of the output of the trace impurity migration code DIVIMP [6]. It describes how much material that is emitted from wall element wk into the plasma ends up on wall element wl . Since the flux of material into the plasma depends on the current surface composition $\delta_{ei,wk}(t)$

and incident particle spectrum $\Gamma_{ej,wl}(t)$ this matrix defines a linear equation system from which the equilibrium $\Gamma_{ej,wl}(t)$ can be calculated given the current $\delta_{ei,wk}(t)$. By combining the differential equation for the surface composition evolution with the linear equation of the flux evolution a differential algebraic equation (DAE) system can be derived that describes the coupled evolution of surface and plasma.

The fact that both the surface processes and the plasma transport processes are described by parameterizations of the calculation results from sophisticated codes allows to couple surface processes and plasma transport without the use of an iterative scheme. This avoids the problems associated with discretizing time or sampling distributions which make iterative schemes prone to artifacts.

The most important input for the impurity transport calculation by DIVIMP is the background plasma. It also defines the constant background plasma flux (D-ions, D-CX) and plasma parameters (T_e , T_i) at the wall. For the JET calculations the background plasma was calculated using a quasi 1D "onion-skin" plasma model (OSM) [12]. While the onion-skin model only solves a simplified version of the Braginskii equations, it allows a very close match to the experimentally observed plasma parameters because measurements of temperature and density at the divertor plates and the outer mid-plane are used as boundary conditions.

For the ITER calculations the approach is slightly different: The near SOL plasma is taken from a SOLPS [13] calculation, while the far SOL plasma is based on a simple isothermal, purely convective plasma model that prescribes plasma parameters that are consistent with observed experimental trends [9]. The differences in the ITER background plasmas can be characterized by several parameters which are summarized in table I. All plasmas have H-mode pedestals but differ in the following parameters: "Sep. distance" is the distance between the primary and secondary separatrix. "Density" is the density in the divertor. "Far SOL T_e/T_i " is the ratio of T_e to the T_i of the majority species (Deuterium). "Far SOL V_{Perp} " is the far SOL convection velocity. "Far SOL T-grad" is an option that switches from an isothermal far SOL to far sol with a T_e gradient. "Near SOL flow" enforces a parallel flow in the background plasma. The so defined background plasmas (see also [9]) span a large range of wall conditions in terms of flux and particle energy.

For both JET and ITER all the background plasmas are defined on a computational grid that tightly matches the entire first wall without gaps. This allows to directly extract wall fluxes around the entire poloidal circumference without the need to extrapolate plasma fluxes across gaps between the calculation grid and the wall. In the DIVIMP calculations the perpendicular transport of impurities is controlled by the perpendicular diffusion coefficient $D_{Perp}(m^2s^{-1})$. In the calculations presented here $D_{Perp} = 1.0 m^2s^{-1}$ was used unless stated otherwise.

3. RESULTS AND DISCUSSION

The main questions that have been addressed in the WallDYN calculations for ITER are the Be deposition in the divertor and the fuel retention by co-deposition. Therefore to judge the predictive significance of the WallDYN calculations, results from JET of Be deposition and

fuel retention are compared to experimental findings in JET during the C-JET and JET-ILW campaigns. The details of these JET-ILW benchmarking calculations are described in [2], only excerpts are shown here.

3.1. WALLDYN MODELING OF JET RESULTS

In Figure 1 the calculated Be deposition flux for the JET-ILW is shown. In the calculations the evolution of the impurity flux and surface composition was followed until they became constant i.e. equilibrium was reached. For all wall elements to equilibrate it typically took ≈ 400 sec of constant ohmic (80295) or H-mode (83559) plasma exposure. It should be noted that not all wall elements reach their equilibrium state equally fast: The higher the local wall flux the faster equilibrium was reached. The final $\eta_{ei,wk} = \frac{\partial \delta e_{i,wk}}{\partial t}$ corresponds to the net erosion ($\eta_{ei,wk} < 0$) or net deposition ($\eta_{ei,wk} > 0$) rate. The main wall is a net Be erosion zone except for some small areas. There is generally no net Be deposition on W divertor targets but a finite Be surface concentration of up to 20%. There is minor Be deposition on the lower part of the inner and outer vertical targets and strong Be deposition on top of tile 1 “apron” (see Figure 1 in [5]). This principal pattern is the same for all background plasma configurations. The absolute deposition rates depend on the presence of additional impurities and on the background plasma type (ohmic, H-mode). Also varying $D_{P_{erp}}$ in the ohmic case from $1.0m^2s^{-1}$ to $10.0m^2s^{-1}$ decreases the Be deposition rate on top of tile 1 “apron” by a factor of ≈ 2 . The reason for this reduction is that a higher $D_{P_{erp}}$ results in less long range transport of Be and thus reduces the amount of Be, eroded at locations far away, that ends up on top of tile 1. Comparing the distribution of Be net deposition and erosion with experimental data from [4, 5] shows good qualitative agreement: Be Deposition dominantly on tile one apron and little Be on the rest of the W divertor area. The actual quantitative numbers on Be layer growth on the tile 1 apron region are the cumulative result of erosion & deposition during many different plasma scenarios. Assuming that the modeled shots are a reasonable proxy for the majority of the JET-ILW plasmas, the experimentally determined layer thickness can be compared to the WallDYN net deposition rates. According to [5] the total divertor time in the initial JET-ILW campaign was $\approx 13h$ and a Be layer thickness of 10 to $15 \pm 5\mu m$ which for a Be density of $\approx 1.0 \times 10^{29}m^{-3}$ results in a Be deposition rate of 2 to $3 \pm 1 \times 10^{19}(m^{-2}s^{-1})$. Compared to the calculated Be deposition rate on tile 1 apron this is lower by factor 3 to 10. Which is not unreasonable since not all of the 13h of divertor time were during steady state plasmas.

Using the ohmic (80295 flat top diverted phase) and H-mode (83559 flat top diverted phase) plasma configuration the D retention rate by co-deposition in equilibrium was calculated. These calculations were performed both for the JET-ILW and JET-C wall material configuration. The resulting retention rates are compared to the experimental data from [8] in Figure 2. The calculation for ohmic and H-mode match the experimental data quite well when long term outgassing is included. As in the experiment the retention in ohmic and H-mode plasmas is roughly a factor 10 lower for the JET-ILW compared to the JET-C material configuration.

3.2. PREDICTIONS FOR ITER

To calculate the Be deposition patterns in ITER for the different background plasmas (see table I) the WallDYN surface model was adopted to also include Be sublimation as an additional loss channel. The steady state surface temperatures at the divertor targets reach temperatures of up to $\approx 1400\text{K}$ where Be sublimation is the dominant loss channel. The main wall was assumed to remain at 385K where sublimation is negligible. WallDYN calculations for different first wall material configurations were performed: A full Be first wall and W divertor with CFC strike point areas = CASE-A, a full Be first wall and a full W divertor = CASE-B and full C first wall and divertor = CASE-C.

In Figure 3 the calculated Be deposition along the ITER poloidal circumference is shown for the ITER reference wall configuration CASE-B (no C). The X-axis is the WallDYN wall element index and along the Y-axis the different background plasma cases are varied. The Be deposition is plotted in units of Be atoms per meter toroidal length (m-tor) and seconds. This value is obtained from the calculated Be deposition flux ($\text{Be} / \text{m}^2 \text{s}$) by multiplying it with the poloidal length of the wall element. The calculation predicts significant Be deposition on upper dump plate and divertor baffles. The reason for the strong deposition at the upper dump plate is the secondary upper X point which in ITER is located close to the upper dump plate. Thus essentially forming two additional strike points on the upper dump with high local fluxes. While this basic deposition pattern is found for all background plasmas, there still exists a strong variation in the absolute Be deposition for different background plasmas. For instance along the inner and outer targets the Be deposition locally varies by almost a factor 10 from the average ($\approx 0.5 \times 10^{19} \text{m} - \text{tor}^{-1} \text{s}^{-1}$) to the maximum ($\approx 3 \times 10^{19} \text{m} - \text{tor}^{-1} \text{s}^{-1}$) deposition rate when averaging over all background plasma cases. This variation in the Be deposition is also found in the fuel retention rate as discussed below.

The fuel retention due to co-deposition in ITER for the different first wall configurations (CASE-A, CASE-B and CASE-C) is shown in Figure 4. There the experimental (from [8]) and calculated JET-ILW and JET-C values together with the extrapolation to ITER are compared. The simulations showed that CASE-B has the lowest retention due to co-deposition whereas CASE-A and CASE-C feature on average a 10 and 100 times higher retention rate respectively. For case C only 100 to 700 full 400 second ITER discharges would be possible before hitting the T-limit of 700g (T:D ratio = 50:50) whereas for CASE-B between 3000 and 20000 full 400 second ITER discharges are possible depending on the plasma configuration. These numbers do not include the influence of cleaning discharges. It should also be noted that the difference between CASE-A and CASE-C is quite small despite the fact that there is much more C in CASE-C. But as the dominant erosion occurs at the C strike points the additional contribution to co-deposition by C eroded from the main wall is small.

These numbers are in line with previous estimates in [14] based on a simple first wall flux scaling. However independent on the wall material configuration, the different background plasmas result in a factor ≈ 10 variation in co-deposition despite similar total wall fluxes. These strong variations

show that a simple wall flux scaling is not enough for predicting retention in ITER for various plasma conditions. Still, for the current ITER material choice (CASE-B) fuel retention by co-deposition will not limit the ITER operation.

During the ITER calculations for the different background plasma cases, excessive W self sputtering was found for certain background plasmas. Scenarios with high edge temperatures/densities result in sputtered W returning to the wall at high charge states ($> 8+$) where they, due to sheath acceleration, result in W self-sputter yields close to unity. This problem is aggravated by the expected oblique ion impact angles. In the calculation oblique impact angles of 40° were chosen based on results and modeling in [15]. The scenarios most prone for excessive self sputtering are those with reduced distance between the primary and secondary separatrix (see table I). The close proximity of the hot plasma to the wall results in a significant increase in the wall flux of high W charge states.

This effect is not expected in current machines, and has not occurred in any other WallDYN calculation performed so far for JET or AUG. The reason is that such a high plasma density combined with a high plasma temperature so close to the wall is not possible in current machines. Therefore no benchmark exists, to test these WallDYN predictions against. None the less these results should not be ignored and be taken into consideration during ITER scenario development.

4. SUMMARY

The global impurity migration code WallDYN has been successfully benchmarked against experimental data on Be migration and co-deposition in both JET-ILW and JET-C material configurations. The calculations qualitatively reproduce the Be deposition patterns from the JET-ILW campaign. A comparison of the calculated retention rate by co-deposition with experimental data from gas balance measurements, even shows quantitative agreement with the experimental retention rates when long term outgassing is taken into account.

Applying the same process physics as for the JET-ILW calculations WallDYN was used to predict Be deposition patterns and the resulting co-deposition for ITER, for a wide range of ITER plasmas conditions. These calculations showed that C leads to unacceptably high retention rates whereas the current ITER material choice (Be main wall and full W divertor) will not limit ITER operation.

These WallDYN calculations have also shown that for certain plasma configuration excessive W self sputtering may occur. Scenarios with a small distance between the primary and secondary separatrix result in eroded W returning to the wall at very high charge states resulting in excessive W self-sputtering. Thus such plasma scenarios may not be possible in ITER.

ACKNOWLEDGMENTS

This work was supported by EURATOM and carried out within the framework of the European Fusion Development Agreement. This work has been carried out within the framework of the

EUROfusion Consortium and has received funding from the European Union's Horizon 2020 research and innovation programme under grant agreement number 633053. The views and opinions expressed herein do not necessarily reflect those of the European Commission. The views and opinions expressed herein do not necessarily reflect those of the ITER Organization.

REFERENCES

- [1]. K. Schmid et al., *Journal of Nuclear Materials* **415** (2011) S284-S288
- [2]. K. Schmid et al., "PSI-2014: Quantitative modeling of fuel retention in the JET-C and JET-ILW wall configurations by WallDYN and predictions for ITER" Submitted to *Journal of Nuclear Materials* (2014)
- [3]. G. De Temmerman et al., *Nuclear Fusion* **48** (2008) 075008
- [4]. K. Heinola et al. "Fuel Retention in JET ITER-Like Wall from Post-Mortem Analysis" Submitted to *Journal of Nuclear Materials* (2014)
- [5]. J.P. Coad et al. *Physica Scripta* **T159**, (2014) 014012
- [6]. P.C. Stangeby, J. D. Elder, *Journal of Nuclear Materials* **196–198** (1992) 258
- [7]. P.C. Stangeby, ISBN 0 7503 0559 2, IOP Publishing Ltd 2000, Chap. 12
- [8]. S. Brezinsek et al., *Nuclear Fusion* **53** (2013) 083023
- [9]. S. Lisgo et al., *Journal of Nuclear Materials* **438** (2013) 580
- [10]. W. Möller, W. Eckstein, J. P. Biersack, *Computer Physics Communications* **51** No. 8, 1988, 355
- [11] A. Mutzke, R. Schneider, W. Eckstein, MPI für Plasmaphysik IPP-Report 12/8, (2011)
- [12] S. Lisgo, P.C. Stangeby, J.D. Elder et al., *Journal of Nuclear Materials* **337** (2005) 256
- [13]. R. Schneider, X. Bonnin, et al., *Contributions to Plasma Physics* **46** (2006) 191
- [14]. J. Roth et. al., *Journal of Nuclear Materials* **390–391**, (2009), 1
- [15]. K. Schmid et al., *Nuclear Fusion* **50** (2010) 105004

Parameter	Range	"Affects"
Sep. distance	10 cm vs 4 cm	Charge states at the wall
Density	Low/Medium/High	Wall fluxes
Far SOL Te/Ti (eV)	Te = 10 Ti = 20 vs. Te = 20 Ti = 40	Erosion rates
Far SOL V_{Perp}	35m/s vs. 100m/s	Far SOL density (impurity screening)
Far SOL T-grad	Off vs. On	Erosion
Near SOL flow	0 vs. 0.5 Mach	Transport to inner divertor

Table I: Parameter differences in the ITER background plasmas and how they "qualitatively affect" the WallDYN solution.

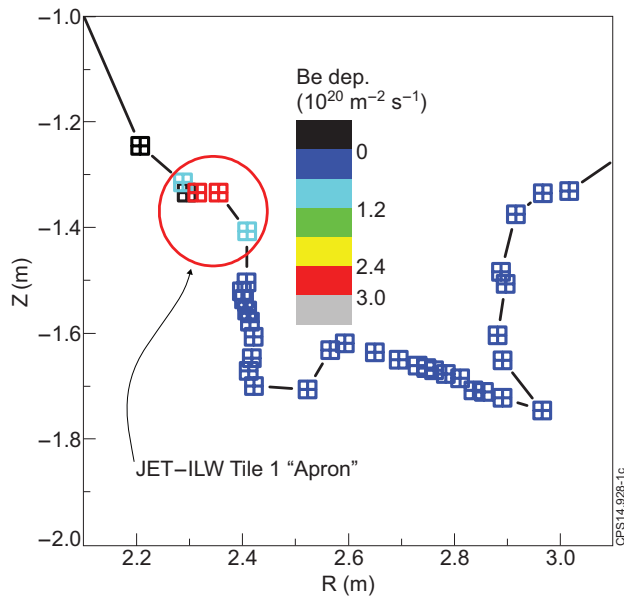


Figure 1: Poloidal variation of Be deposition in JET-ILW configuration.

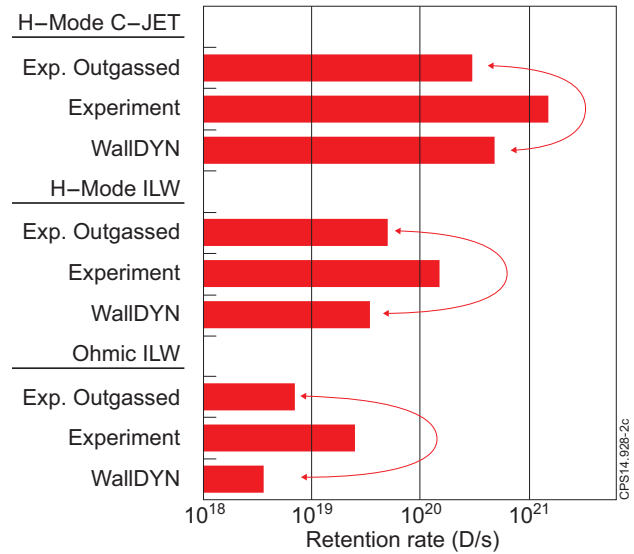


Figure 2: Comparison of WallDYN calculated retention rates with experimental results for different plasma configurations. The red arrows denote experimental and calculated values that can be compared directly.

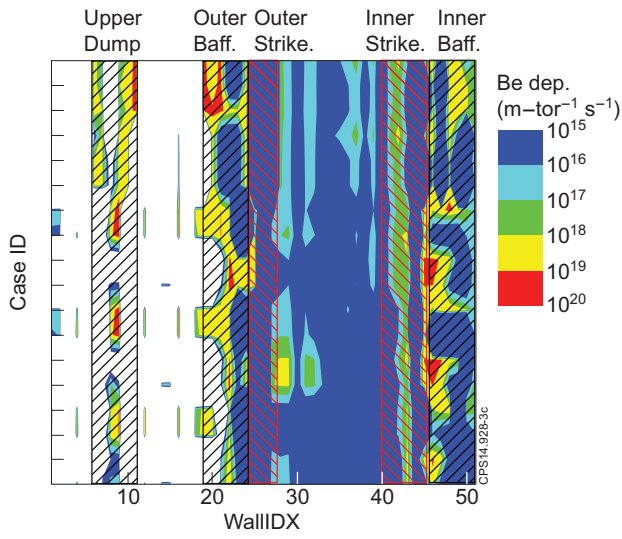


Figure 3: Comparison of WallDYN calculated Be deposition along the ITER poloidal circumference. The different background plasmas (see also Table 1) varies along the Vertical axes.

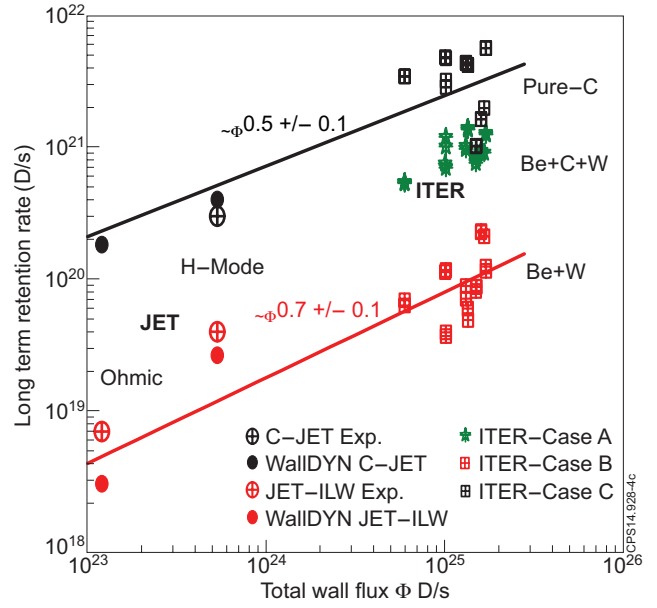


Figure 4: Comparison of WallDYN calculated retention rates for ITER and JET. Black: Pure C, Green: C+Be+W, Red: Be+W.